Journal of Marine Science and Technology

Volume 27 | Issue 4 Article 7

INTEGRATED NUMERICAL MODEL FOR THE SIMULATION OF THE T.S. TAIPEI OIL SPILL

Cheng-Di Dong
Departmentof Marine Environmental Engineering, National Kaohsiung University of Science and Technology, Kaohsiung City, Taiwan, R.O.C.

Thi-Hong-Hanh Nguyen
Institute of Marine Science and Technology, National Kaohsiung University of Science and Technology, Kaohsiung City, Taiwan, R.O.C

Tien-Hung Hou
Departmentof Marine Environmental Engineering, National Kaohsiung University of Science and Technology, Kaohsiung City, Taiwan, R.O.C

Chia-Cheng Tsai
Departmentof Marine Environmental Engineering, National Kaohsiung University of Science and Technology, Kaohsiung City, Taiwan, R.O.C.Center of Excellence for Ocean Engineering, National Taiwan Ocean University, Keelung, Taiwan, R.O.C. Department of Marine Environment and Engineering, National Sun Yat-senUniversity, Kaohsiung, Taiwan, R.O.C., tsaichiacheng@nkust.edu.tw

Recommended Citation

Dong, Cheng-Di; Nguyen, Thi-Hong-Hanh; Hou, Tien-Hung; and Tsai, Chia-Cheng (2019) "INTEGRATED NUMERICAL MODEL FOR THE SIMULATION OF THE T.S. TAIPEI OIL SPILL," *Journal of Marine Science and Technology*: Vol. 27: Iss. 4, Article 7.
DOI: 10.6119/JMST.201908_27(4).0007
Available at: https://jmstt.ntou.edu.tw/journal/vol27/iss4/7

INTEGRATED NUMERICAL MODEL FOR THE SIMULATION OF THE T.S. TAIPEI OIL SPILL

Acknowledgements

The authors wish to acknowledge the Coastal Water and Environment Center, College of Ocean Engineering, National Kaohsiung University of Science and Technology for their support of this study.

Journal of Marine Science and Technology, Vol. 27, No. 4, pp. 359-368 (2019)
DOI: 10.6119/JMST.201908_27(4).0007

INTEGRATED NUMERICAL MODEL FOR THE SIMULATION OF THE *T.S. TAIPEI* OIL SPILL

Cheng-Di Dong[1], Thi-Hong-Hanh Nguyen[2], Tien-Hung Hou[1], Chia-Cheng Tsai[1,3,4]

Key words: oil spill, oil spill model, openoil, Princeton Ocean Model (POM).

ABSTRACT

In this study, two freely available models, the hydrodynamic model Princeton Ocean Model (POM) and the oil spill model OpenOil, are integrated to simulate the *T.S. Taipei* oil spill that occurred on March 10, 2016. In these models, the amount of oil spilled into the sea is distributed among a large number of small and equal mass particles. Meteorological data such as wind velocity, air surface temperature, and current data from the POM are used as inputs. The Lagrangian particle traction with prescribed advection and reaction is used to model the spilled oil. The results are compared with *in-situ* observations and simulation results from the Oil Modeling Application Package (OILMAP), and a qualitative agreement was found. This demonstrates that the proposed integrated model can be a useful tool to predict the impact of oil spills on the marine environment.

I. INTRODUCTION

An oil spill is the release of liquid petroleum hydrocarbon into the environment due to human activities such as marine oil transport, marine oil exploration, and underwater oil pipelines. Statistical data from the International Tanker Owners Pollution Federation Limited (ITOPF) show that there were 592 spills of 7 tons or more worldwide from 1990 to 2017 (ITOPF, 2018). These oil spills have serious effects on the environment, economy, and society (Corn, 2010; Hagerty, 2010; Lin and Mendelssohn, 2012). The fate of spilled oil depends on the environmental conditions and the behavior of the oil itself. The behavior of the spilled oil can be divided into transport (trajectory) processes, which are determined by advection and turbulent diffusion, and fate (weathering) processes, which include spreading, evaporation, dispersion, dissolution, emulsification, oil-shoreline interaction, biodegradation, and sedimentation (Fig. 1). All these processes are interrelated, and the complicated nature of oil spills makes it difficult for decision-makers to respond to them, which they need to do quickly and effectively to reduce their impact. As a result, oil spill models are required to predict the transport and fate of the oil.

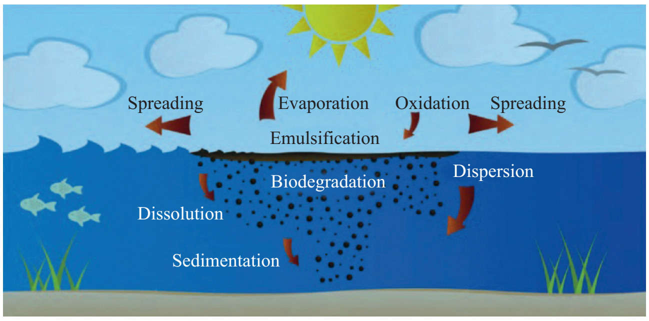

Fig. 1. Weathering processes.

The last three decades have witnessed the evolution of spill models and their widespread use in spill response and impact assessment (Spaulding, 2017). Most early models could simulate only a few processes (Reed et al., 1999) and were thus employed in more straightforward but less accurate approaches. Currently, with better knowledge of oil transport and the fate of spilled oil, there have been improvements in ocean and atmospheric models, which provide more accurate inputs for oil spill models. Moreover, the development of computing technology has enabled spill models to process complicated simulations efficiently.

A number of oil spill models are widely used by private companies, research institutes, and governments, such as ADIOS (National Oceanic and Atmospheric Administration [NOAA], 1994), GNOME (Beegle-Krause, 2001), SLROSM (Belore, year unknown), OILMAP (also with SARMAP and SIMAP, Applied Science Associate (ASA), 1997; ASA, 2004), OSCAR (Reed et al., 1995a; Reed and Rye, 1995b; Aamo et al., 1997; Reed et al., 2001), GULFSPILL (Al-Rabeh et al., 2000), MEDSLIK (Zodiatis et al., 2012), MEDSLIK-II (De Dominicis et al., 2013-Part 1; De Dominicis et al., 2013-Part 2), POSEIDON-OSM

Paper submitted 11/30/18; revised 04/19/19; accepted 05/24/19. Author for correspondence: Chia-Cheng Tsai (e-mail: tsaichiacheng@nkust.edu.tw).
[1] *Departmentof Marine Environmental Engineering, National Kaohsiung University of Science and Technology, Kaohsiung City, Taiwan, R.O.C.*
[2] *Institute of Marine Science and Technology, National Kaohsiung University of Science and Technology, Kaohsiung City, Taiwan, R.O.C.*
[3] *Center of Excellence for Ocean Engineering, National Taiwan Ocean University, Keelung, Taiwan, R.O.C.*
[4] *Department of Marine Environment and Engineering, National Sun Yat-sen University, Kaohsiung, Taiwan, R.O.C.*

(Annika et al., 2001; Nittis et al., 2006), OILTRANS (Berry et al., 2012), SEATRACK WEB (Ambjörn et al., 2011), and MOTHY (Daniel, 1996; Daniel et al., 2003). Most of these are commercial software, so the source code is unavailable to users for modification and improvement.

In this study, the freely available oil spill simulation model OpenOil, which is a sub-model of OpenDrift, is utilized. This model is programmed in Python and was developed at the Norwegian Meteorological Institute (Dagestad et al., 2017). The Princeton Ocean Model (POM; (Mellor, 1998) was used to determine the distribution of the sea currents. Because both models are open-source, they can be modified by users to support their needs. These models were applied to an oil spill incident in Northern Taiwan involving the container ship *T.S. Taipei*. The results are compared with *in-situ* observations and simulation results from OILMAP.

II. THEORY AND METHODOLOGY

1. The Lagrangian Trajectory Model

In the Lagrangian trajectory model, oil spilled on the sea surface is computed as a large number of small particles of equal mass under the influence of velocity fields as part of oceanic and atmospheric circulation. The coordinates X, Y, and Z for the oil particles can be calculated as follows (Wang et al., 2008):

$$\frac{dX}{dt} = u + u', \frac{dY}{dt} = v + v', \quad \frac{dZ}{dt} = w + w' + u_L \tag{1}$$

where $\langle u(x, y, z, t)\rangle$, $\langle v(x, y, z, t)\rangle$, and $\langle w(x, y, z, t)\rangle$ are the drift velocities of the oil particles, representing the drift caused by the combined effect of the wind, current, and waves, not only on the surface layer but also in the water column; $\langle u'(x, y, z, t)\rangle$, $\langle v'(x, y, z, t)\rangle$, and $\langle w'(x, y, z, t)\rangle$ are the turbulent fluctuations of the velocity which simulate the turbulent diffusion of the oil droplets; and u_L is the buoyancy velocity of oil droplets.

2. Governing Equations for Ocean Current

The water current has an important effect on both advection and the spread of the oil slick; in this study, it was derived using the POM. This model uses a curvilinear orthogonal grid for the horizontal coordinates and a sigma grid for the vertical coordinates. The governing equations are listed below.

Internal mode:

$$\frac{\partial DU}{\partial x} + \frac{\partial DV}{\partial y} + \frac{\partial \omega}{\partial \sigma} + \frac{\partial \eta}{\partial t} = 0 \tag{2}$$

$$\frac{\partial UD}{\partial t} + \frac{\partial U^2 D}{\partial x} + \frac{\partial UVD}{\partial y} + \frac{\partial U\omega}{\partial \sigma} - fVD + gD\frac{\partial \eta}{\partial x} = \frac{\partial}{\partial \sigma}\left[\frac{K_M}{D}\frac{\partial U}{\partial \sigma}\right] + \frac{\partial}{\partial x}\left[2A_M D\frac{\partial U}{\partial x}\right] + \frac{\partial}{\partial y}\left[A_M D\left(\frac{\partial U}{\partial y} + \frac{\partial V}{\partial x}\right)\right] \tag{3}$$

$$\frac{\partial VD}{\partial t} + \frac{\partial UVD}{\partial x} + \frac{\partial V^2 D}{\partial y} + \frac{\partial V\omega}{\partial \sigma} + fUD + gD\frac{\partial \eta}{\partial y} = \frac{\partial}{\partial \sigma}\left[\frac{K_M}{D}\frac{\partial V}{\partial \sigma}\right] + \frac{\partial}{\partial y}\left[2A_M D\frac{\partial V}{\partial y}\right] + \frac{\partial}{\partial x}\left[A_M D\left(\frac{\partial U}{\partial y} + \frac{\partial V}{\partial x}\right)\right] \tag{4}$$

$$\frac{\partial q^2 D}{\partial t} + \frac{\partial Uq^2 D}{\partial x} + \frac{\partial Vq^2 D}{\partial y} + \frac{\partial \omega q^2}{\partial \sigma} = \frac{\partial}{\partial \sigma}\left[\frac{K_q}{D}\frac{\partial q^2}{\partial \sigma}\right] + \frac{2K_M}{D}\left[\left(\frac{\partial U}{\partial \sigma}\right)^2 + \left(\frac{\partial V}{\partial \sigma}\right)^2\right] + \frac{2g}{\rho_0}K_H\frac{\partial \tilde{\rho}}{\partial \sigma} - \frac{2Dq^3}{B_1 l} + \frac{\partial}{\partial x}\left(DA_H\frac{\partial q^2}{\partial x}\right) + \frac{\partial}{\partial y}\left(DA_H\frac{\partial q^2}{\partial y}\right) \tag{5}$$

$$\frac{\partial q^2 lD}{\partial t} + \frac{\partial Uq^2 lD}{\partial x} + \frac{\partial Vq^2 lD}{\partial y} + \frac{\partial \omega q^2 l}{\partial \sigma} = \frac{\partial}{\partial \sigma}\left[\frac{K_q}{D}\frac{\partial q^2 l}{\partial \sigma}\right] + E_1 l - \frac{Dq^3}{B_1}\left(\frac{K_M}{D}\left[\left(\frac{\partial U}{\partial \sigma}\right)^2 + \left(\frac{\partial V}{\partial \sigma}\right)^2\right] + E_3\frac{g}{\rho_0}K_H\frac{\partial \tilde{\rho}}{\partial \sigma}\right)\tilde{W} + \frac{\partial}{\partial x}\left(DA_H\frac{\partial q^2 l}{\partial x}\right) + \frac{\partial}{\partial y}\left(DA_H\frac{\partial q^2 l}{\partial y}\right) \tag{6}$$

where ω is the velocity component normal to the sigma surfaces; A_M is the horizontal diffusivity; E_1, E_3, and B_1 are close constants for internal mode; $q^2/2$ is the kinetic energy of the turbulence; $q^2 l$ is the length scale of the turbulence, ρ is the density of seawater, and K_M, K_H, K_q are turbulent close parameters given by Mellor (1998).

External mode:

$$\frac{\partial \eta}{\partial t} + \frac{\partial D\bar{U}}{\partial x} + \frac{\partial D\bar{V}}{\partial y} = 0 \tag{7}$$

$$\frac{\partial D\bar{U}}{\partial t}+\frac{\partial D\bar{U}^2}{\partial x}+\frac{\partial D\bar{U}\bar{V}}{\partial y}-fD\bar{V}+gD\frac{\partial \eta}{\partial x}$$
$$=-wu(0)+wu(-1)+\frac{\partial}{\partial x}\left[2\bar{A}_M D\frac{\partial \bar{U}}{\partial x}\right] \quad (8)$$
$$+\frac{\partial}{\partial y}\left[\bar{A}_M D\left(\frac{\partial \bar{U}}{\partial x}+\frac{\partial \bar{V}}{\partial y}\right)\right]$$

$$\frac{\partial D\bar{V}}{\partial t}+\frac{\partial D\bar{U}\bar{V}}{\partial x}+\frac{\partial D\bar{V}^2}{\partial y}+fD\bar{U}+gD\frac{\partial \eta}{\partial y}$$
$$=-wv(0)+wv(-1)+\frac{\partial}{\partial y}\left[2\bar{A}_M D\frac{\partial \bar{V}}{\partial y}\right] \quad (9)$$
$$+\frac{\partial}{\partial x}\left[\bar{A}_M D\left(\frac{\partial \bar{U}}{\partial y}+\frac{\partial \bar{V}}{\partial x}\right)\right]$$

The overbars denote vertically integrated velocities such as

$$\bar{U}\equiv\int_{-1}^{0}Ud\delta .$$

3. Advection Velocity

Spilled oil drifts on the surface due to the combined action of the wind, current, and waves. Based on (Zhang et al., 1991), the drift velocity can be written as:

$$u=\alpha_w Du_w+\alpha_c u_c+u_{wave},$$
$$v=\alpha_w Dv_w+\alpha_c v_c+u_{wave}, \quad (10)$$
$$w=w_c$$

where u_w and v_w are the wind velocities at 10 m above the water surface; u_c, v_c, and w_c are the velocities of the surface water current, which can be obtained from the POM; u_{ware} is the wave-induced velocity, α_w is the wind drift factor, which is usually taken as 0.03 (Stolzenbach et al., 1977); α_c is a factor that accounts for the contribution of the drift of the oil slick on the water surface due to the current; and D is the transformation matrix that allows the deviation angle to be introduced (Zhang et al., 1991):

$$D=\begin{Bmatrix} cos\theta & sin\theta \\ -sin\theta & cos\theta \end{Bmatrix} \quad (11)$$

where $\theta=40^o-8\sqrt[4]{u_w^2+v_w^2}$ if $0\le\sqrt{u_w^2+v_w^2}\le 25$ m/s $\theta=0^o$ if m/s.

4. Turbulent Diffusion

Turbulent diffusive transport is generally simulated using the random walk technique. The fluctuation velocity components u', v', and w' can be written as follows (Fischer et al., 1979):

$$u'=R_n\sqrt{4K_\alpha/\Delta t}cos(\phi)$$
$$v'=R_n\sqrt{4K_\alpha/\Delta t}sin(\phi) \quad (12)$$
$$w'=R_n\sqrt{2K_z/\Delta t}$$

where Δt is the time step, R_n is a normally distributed random number with a mean value of 0 and a standard deviation of 1, ϕ is the directional angle, which is assumed to be a uniformly distributed random angle in the range 0 – π, and K_α is the turbulent diffusivity in the α-direction (α = x, y) (Sayre, 1968). In the vertical direction, K_z can be calculated using the equation below (Johansen, 1982):

$$K_z=0.028\left[\frac{H_s^2}{T}\right]e^{-2kz} \quad (13)$$

where T is the wave period, k is the wave number, and z is the vertical coordinates for the oil droplets.

5. Stokes Drift

According to Breivik et al. (2016), the Stoke drift velocity profile under a Phillips-type spectrum can be determined as follows:

$$V=\frac{v_0}{2k_p}(1-2\beta/3) \quad (14)$$

where β = 1 for the Phillips spectrum; v_0 is the surface Stokes drift velocity, and k_p is the peak wave number.

If the transport and surface Stokes drift are known, the assumption that the Phillips spectrum is a good representation of the Stokes drift can be used to determine an inverse depth scale k by substituting it for the peak wave number k_p:

$$\bar{k}=\frac{v_0}{2V}(1-2\beta/3) \quad (15)$$

6. Oil Droplet Entrainment

According to Li et al. (2017), the rate of oil entrainment from the slick to the mixing layer is a function of the dimensionless Weber (We) and Ohnesorge (Oh) numbers as follows:

$$Q=4.604.10^{-10}.We^{1.805}Oh^{-1.023}F_{bw} \quad (16)$$

The Weber number describes the relative importance of the inertial forces and oil–water interfacial tension:

$$We=\frac{\rho_w gH_s d_0}{\rho_{0-w}} \quad (17)$$

where ρ_w is the seawater density, g is the acceleration due to gravity, H_s is the significant wave height, σ_{0-w} is the oil-water interfacial tension, and d_0 is the Rayleigh-Taylor instability maximum diameter that is given by the following:

$$d_0 = 4\sqrt{\frac{\sigma_{0-w}}{g(\rho_w - \rho_0)}} \quad (18)$$

The Ohnesorge number describes the ratio of viscous forces to the inertial and surface tension forces.

$$Oh = \frac{\mu_0}{\sqrt{(\rho_0 \sigma_{0-w} d_0)}} \quad (19)$$

where μ_0 is the dynamic oil viscosity.

The fraction of the sea surface covered by breaking waves per unit of time, F_{bw}, is given as follows (Delvigne and Sweeney, 1988):

$$F_{bw} = \begin{cases} c_b \cdot \dfrac{U_{10m} - U_0}{T_p} & \text{if } U_{10m} > U_0, \\ 0 & \text{otherwise,} \end{cases} \quad (20)$$

where $c_b = 0.032sm^{-1}$ is a constant, U_{10m} is the wind speed 10 m above the sea surface, $U_0 = 5sm^{-1}$, and T_p is the peak (or significant) wave period.

7. Oil Droplet Size Distribution

The droplet size distribution can be expressed either as a number-based or a volume-based particle size distribution (Johansen et al., 2015). The number-based (N) particle size distribution is described using the median droplet diameter:

$$D_{50}^{N} = AhWe^{-a} + Bh\,\mathrm{Re}^{-b} \quad (21)$$

where h is the oil film thickness (m), A and B are empirical coefficients (A =2.252 and B = 0.027), and a and b are exponents ($a = b = 0.6$). The Reynolds number and Weber number for equation (18) are given by:

$$\mathrm{Re} = \frac{\rho_0 h\sqrt{gH}}{\mu}$$
$$We = \frac{\rho_0 hgH}{\sigma_{0-w}} \quad (22)$$

where H is the fall height for oil droplets in free-fall (plunging) wave tank experiments, which has been found to be equivalent to the wave height (Reed et al., 2009)

The volume size median diameter, D_{50}^{V}, can be computed with the Hatch-Chaote conversion equation (Johansen et al., 2015):

$$\ln D_{50}^{V} = \ln D_{50}^{N} + 3(s\ln 10)^2 \quad (23)$$

where s is the logarithmic base-10 standard deviation. From experiments, s = 0.38 ± 0.05.

8. Weathering

In conjunction with the vertical and horizontal drifts, the weathering of the spilled oil should also be considered. OpenOil interacts with the already existing computational library OilLibrary, which was developed by NOAA (https://github.com/NOAA-ORR-ERD/OilLibrary) (Lehr et al., 2002). Also being open source and written in Python, OpenOil can be integrated with the NOAA's OilLibrary in a straightforward manner (Dagestad et al., 2017).

To calculate evaporation, the model uses the pseudo-component approach (Jones, 1997). The rate of evaporation depends on the oil properties and wind speed. With some oil types, 20%-40% of the mass is evaporated within the first 6-12 hours, while some do not evaporate at all. In the process of water dispersing into oil in the form of water droplets, Fingas's model (Fingas and Fieldhouse, 2009) is used to estimate the water content and viscosity of the resulting water-in-oil state and the time of formation. Not all oils form water-in-oil emulsions and many crude oils only start to emulsify after some of the components have evaporated (Fingas, 2016).

In addition to the state-of-the-art parameterizations of processes such as evaporation, emulsification, and dispersion, this library consists of a database of the measured properties of almost 1000 oil types from around the world, which is crucial for obtaining accurate results due to the vastly different properties of oil from different sources/wells.

III. APPLICATION OF THE MODEL TO THE OIL SPILL ACCIDENT OF *T.S. TAIPEI*

The model is used to simulate the *T.S Taipei* oil spill, which occurred in Northern Taiwan. Simulations of the oil slicks that occurred after the spill are presented and discussed.

1. The Incident

On March 10, 2016, at around 10 a.m. local time, a 15,487 GT container ship, the *T.S. Taipei*, registered in Taiwan, lost power as a result of engine failure in northern coastal waters as a result of a strong northeastern winter monsoon. It was carrying a total of 505 m^3 of fuel and oil (411, 42, and 52 m^3 of fuel, diesel, and lubricant, respectively) as well as 392 cargo containers (149 on deck and 243 in the cargo holds), including 9 containing hazardous substances (Kai et al., 2017).

In this area, the northeastern winter monsoon creates rough seas. For example, the waves can be as high as 6 m and the winds can reach level 12. In these inclement weather conditions, on March 24, 2016, *T.S. Taipei* ran aground 400 m from the northern

Table 1. Stations used for model validation.

Stations	North latitude	East longitude
Linshanbi	25°17′02″	121°30′37″
Keelung	25°09′18″	121°45′08″

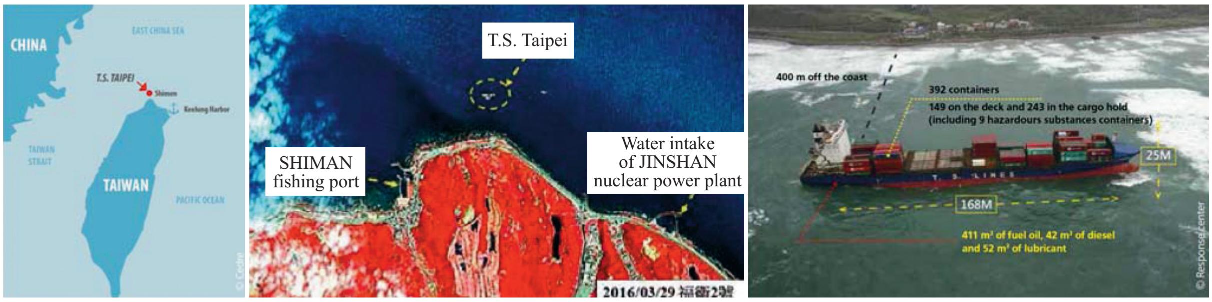

Fig. 2. Incident site location.

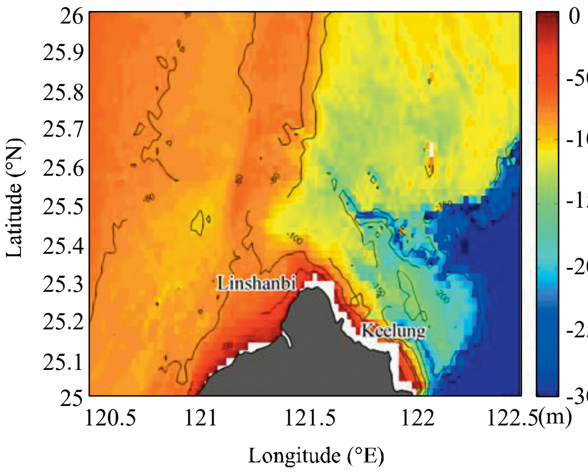

Fig. 3. Bathymetry at the incident site.

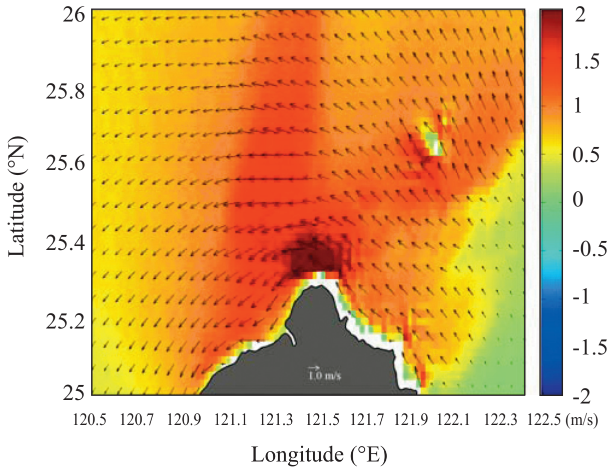

Fig. 4. Computational tidal currents on March 25 at 14:00.

tip of Shimen and was split in two parts, causing a massive oil spill of about 40 tons of heavy fuel oil. Fig. 2 presents the incident ground site.

The site location is a highly sensitive environment, including fishing areas, tourist attractions, and two nuclear power plants. To reduce the impact, the Environmental Protection Administration (EPA) of Taiwan requested that one of Taiwan's satellites, FORMOSAT-2, begin monitoring the seas to provide the response teams with real-time data on the changes in sea conditions in the vicinity of the incident. The EPA also used unmanned aerial vehicles (UAVs) and land-based radar to monitor the marine pollution. The oil dispersal simulation modeling system (OILMAP) was used to predict the impact of the oil slick on the surrounding areas.

2. The Input Data

The computational domain is shown in Fig. 3. The hydrodynamic model is driven by wind stress, sea surface height, and vertical velocity. Whereas both the vertical velocity field and sea surface height are interpolated using Hybrid Coordinate Ocean Model (HYCOM) data, the wind stress is interpolated using Satellite Wind at the ocean surface. In this work, the POM is implemented with a horizontal grid resolution of 1/50° and 31 vertical sigma levels.

Data for tidal currents from the POM, which is validated using data from the 2016 tide tables at two prediction stations (Table 1), and wind field data from the Fugui Cape buoy, which was obtained from the Central Weather Bureau (CWB), are used as input data. The duration of the simulation is 108 hours, starting from March 24, 2016 at 13:00 UTC when the spill occurred. It is assumed from observations that 40,000 oil particles were released over a period of 6 hours. The input data are summarized in Table 2.

3. Results and Discussion

The simulated current field for March 25, 2016 (1 day after the oil spill) is shown in Fig. 4 (high tide) and Fig. 5 (low tide). The tide current speed peaks at around 25°19′N 121°33′E,

Table 2. Input parameters for sample simulation.

Parameter	Value
Position (Longitude and latitude)	25°18′05″N 121°34′35″E
Start Time (The time the oil was spilt)	2016/03/24 13:00 UTC
Simulation Length	108 hours
Oil Type	IFO 300
Oil Spill Amount	40 tons
Sea Temperature	19°C
Model Time Interval	30 minutes
Output Time Interval	30 minutes
Number of Particles	40,000
Wind Factor	3.5 %

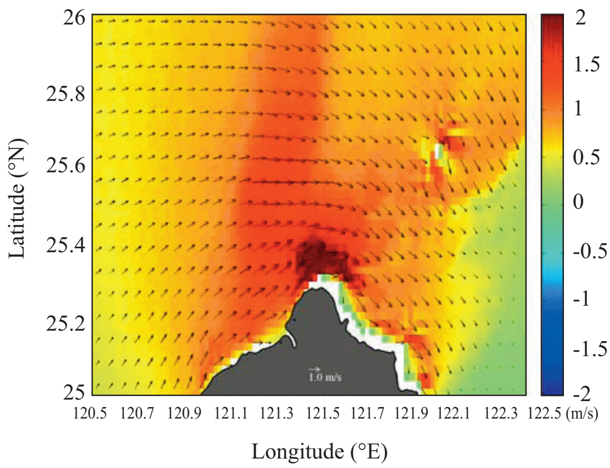

Fig. 5. Computational tidal currents on March 25 at 20:00.

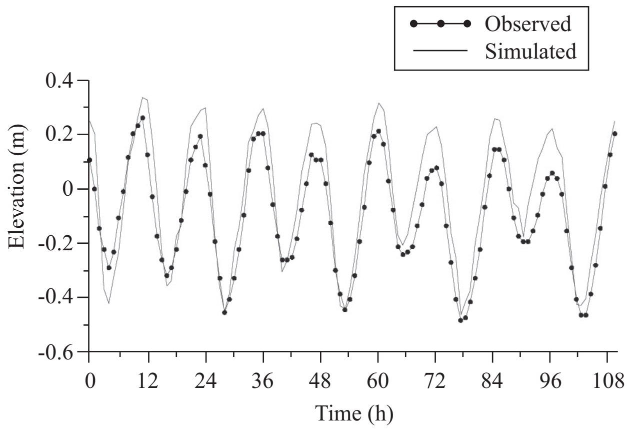

Fig. 7. Comparison of the elevation taken simulations and observations at Keelung Station.

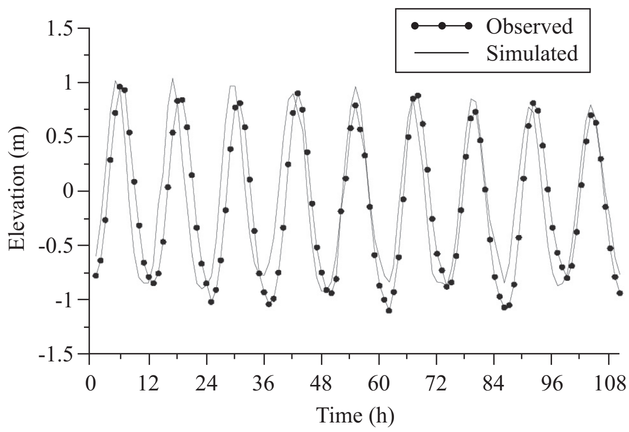

Fig. 6. Comparison of the elevation taken from simulations and observations at Linshanbi Station.

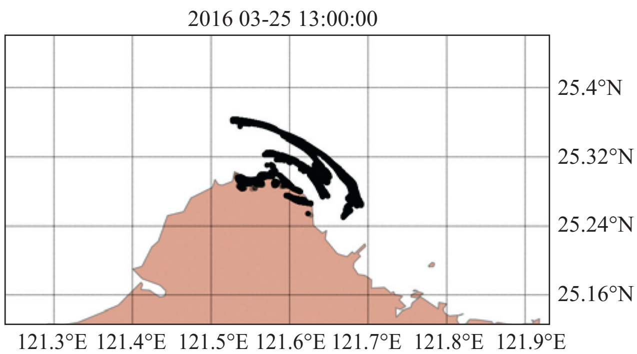

Fig. 8. Simulation results at 13:00 on March 25 (24 hours after the oil spill).

which generally coincides with the incident location. The tide current can have a significant influence on the spread of the spilled oil. Figs. 6 and 7 compare the time history records of the water surface elevation simulated using the POM and data from the tide tables at the Linshanbi and Keelung stations. It is clear that the elevation produced by the numerical model is in good agreement with the observed elevations.

The movement of the oil slick on the surface after 24 hours and 108 hours is shown in Figs. 8 and 9, respectively. An image from the satellite COSMO-SkyMED (Fig. 10(a)) shows a long

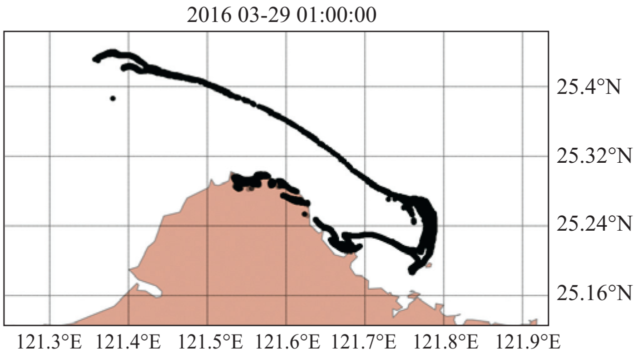

Fig. 9. Simulation results at 01:00 on March 29 (108 hours after the oil spill).

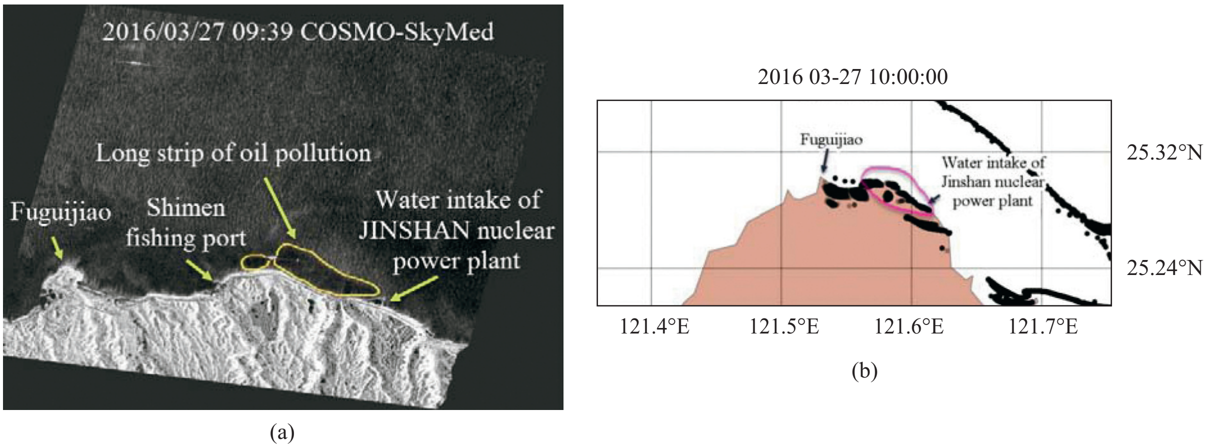

Fig. 10. Comparison between (a) a COSMO-SkyMed image and (b) the present simulation.

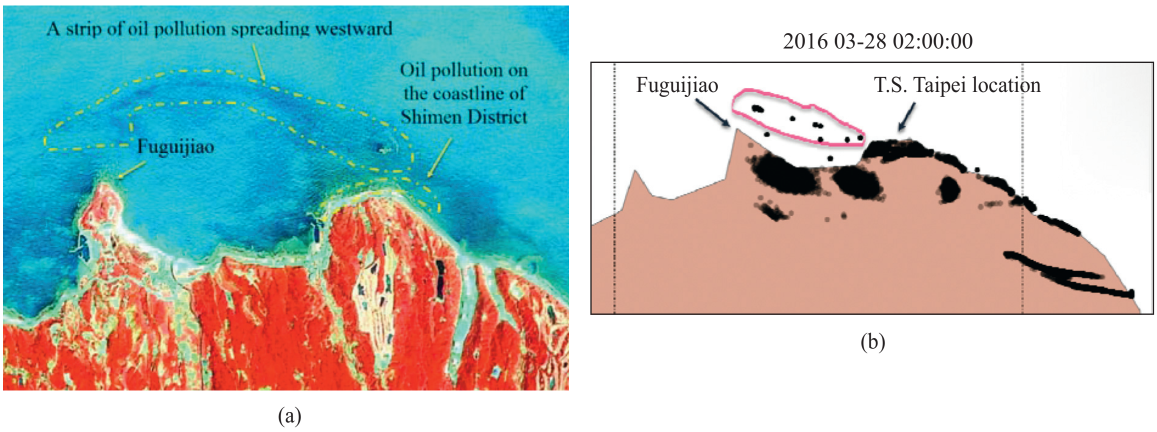

Fig. 11. Comparison between (a) a COSMO-SkyMed image and (b) the present simulation.

oil slick (about 4 km in length and 1 km in width) spreading eastward on March 27 at 09:39. The oil had reached the water intake of the Jinshan nuclear power plant. The proposed simulation produces similar results (Fig. 10(b)). Based on information from the Taiwanese satellite FORMOSAT-2, it was observed that a strip (4 km in length and 100 m in width) of oil had spread westward at 02:00 on March 28 (Fig. 11(a)). This agrees with the results of the proposed model simulation in Fig. 11(b). Fig. 12 presents a comparison between the images from UAVs, FORMOSAT-2, and the simulation results at the final time stage, with all three images showing similar areas of affected coastline.

In comparison with the results of the proposed model presented in Fig. 10, the OILMAP results (Fig. 13) showed that the spilled oil had been transported further southward along the coastline

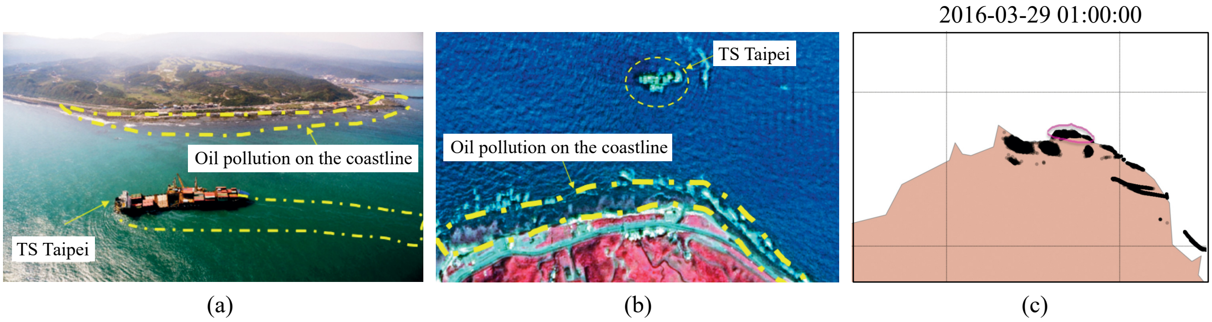

Fig. 12. Images from (a) unmanned aerial vehicles (UAVs) at 02:24 and (b) FORMOSAT 2 at 02:03 compared to (c) the simulation results at 01:00 on March 29, 2016.

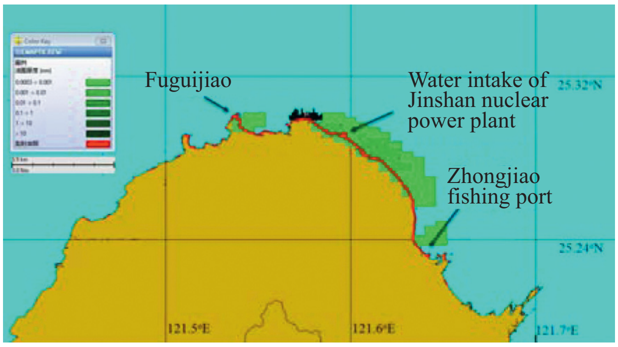

Fig. 13. The results of the OILMAP simulation at 10:00 on March 27.

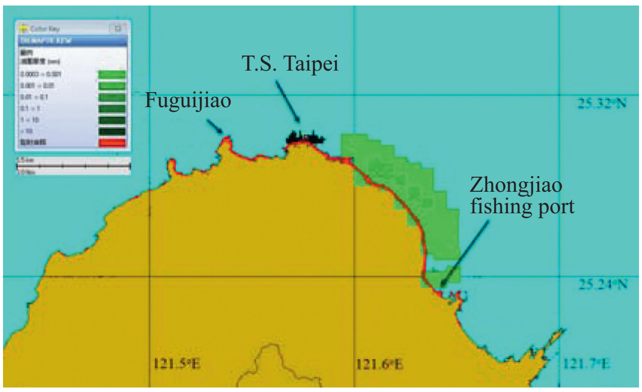

Fig. 14. The results of the OILMAP simulation at 02:00 on March 28.

of Shimen, reaching Zhongjiao Fishing Port. On March 28 at 02:00, the OILMAP simulation (Fig. 14) does not show any oil on the sea between the ship location and Fuguijiao, unlike what is displayed in Fig. 11(a), but the affected coastal area in both simulations (Fig. 11(b) and Fig.14) are similar. In this case, the proposed integrated model thus produces slightly better results, although the OILMAP prediction obtained current data from the Hydrodynamic Modeling System (HYDROMAP), which has a higher resolution than the POM.

Fig. 15 shows the vertical distribution of oil droplets after 12 h, 24 h, and 48 h. Unfortunately, no observed vertical distribution of the oil slick particles is available for comparison.

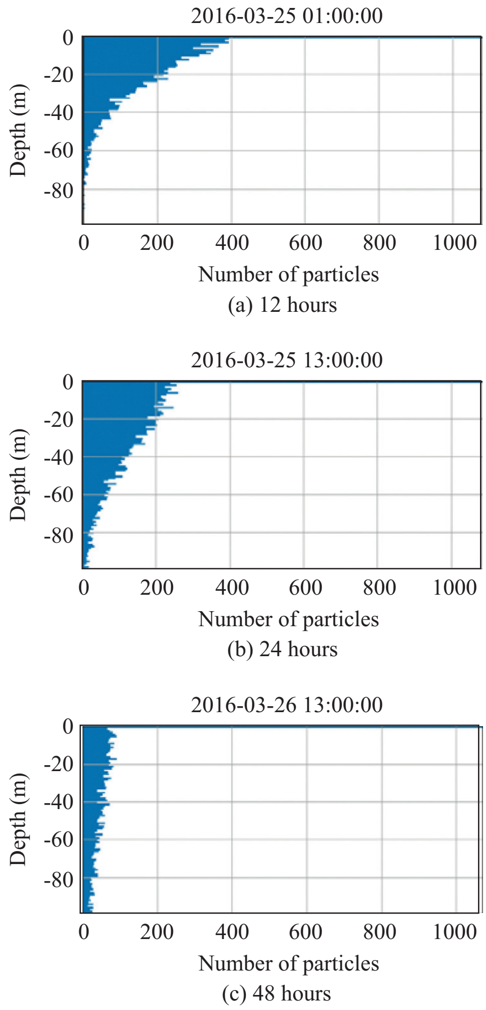

Fig. 15. Vertical distribution of oil droplets simulated in the water column after (a) 12 hours, (b) 24 hours, and (c) 48 hours.

However, these results indicate that it is possible to use this open-source model for 3-D oil spill simulations.

IV. CONCLUSIONS

An integrated model for simulating oil spills is presented in this paper. The model, named OpenOil, is based on a Lagrangian particle approach, which regards an oil slick as the movement of a large number of individual particles. The movement of particles is driven by the water currents on the surface. The random walk technique is used for horizontal diffusion. The weathering processes for spilled oil, including emulsification, dispersion, and evaporation, in OpenOil interface with the NOAA's Oil-Library. The POM was developed to provide hydrodynamic parameters for the ocean currents. Both the hydrodynamic and oil spill models are publicly available, so it is possible for users to modify, improve, and adapt the model for their own requirements.

The integrated model was used to simulate the oil spill incident involving *T.S. Taipei*. The simulated trajectories of the spilled oil slick agree with not only the observed data from satellites (FORMOSAT-2 and COSMO-SkyMed) and UAVs but also the simulation results from the commercial software OILMAP. Simulations of the vertical movement of the particles are not verified because there were no observation data available for a comparison to be made. In general, the results of the present study demonstrate that the proposed model (which integrates the freely available hydrodynamic POM and the oil spill model OpenOil) can be a useful tool for predicting the effect of oil spills on the marine environment.

ACRONYMS

ADIOS	Automated Data Inquiry for Oil Spills
ASA	Applied Science Associate
CWB	Centre Weather Bureau
GNOME	General NOAA Operational Modeling Environment
ITOPF	International Tanker Owners Pollution Federation Limited
MOTHY	Modèle Océanique de Transport d'Hydrocarbures
NOAA	National Oceanic and Atmospheric Administration
OILMAP	Oil Modeling Application Package
OSCAR	Oil Spill Response and Contingency Model
POM	The Princeton Ocean Model
POSEIDO-OSM	POSEIDO Oil Spill Model
SARMAP	Search & Rescue Model Application Package
SIMAP	Spill Impact Model Application Package
SLROSM	SL Ross Oil Spill Fate and Behavior Model
UAV	Unmanned Aerial Vehicle

ACKNOWLEDGEMENTS

The authors wish to acknowledge the Coastal Water and Environment Center, College of Ocean Engineering, National Kaohsiung University of Science and Technology for their support of this study.

REFERENCES

Aamo, O. M., M. Reed and K. Downing (1997). Oil spill contingency and response (OSCAR) model system: sensitivity studies. Proceedings of International Oil spill conference, Florida, USA, 429-438.

Al-Rabeh, A., R. Lardner and N. Gunay (2000). Gulfspill Version 2.0: a software package for oil spills in the Arabian Gulf. Environmental Modelling & Software 15, 425-442.

Ambjörn, C., O. Liungman, J. Mattsson and B. Håkansson (2011). Seatrack Web: the HELCOM tool for oil spill prediction and identification of illegal polluters. In: Oil Pollution in the Baltic Sea, edited by A. G. Kostianoy, Lavrova, Olga Yu, Springer, 155-183.

Annika, P., T. George, P. George, N. Konstantinos, D. Costas and C. Koutitas (2001). The Poseidon operational tool for the prediction of floating pollutant transport. Marine Pollution Bulletin 43, 270-278.

Beegle-Krause, J. (2001). General NOAA oil modeling environment (GNOME): a new spill trajectory model. Proceedings of International Oil Spill Conference, Florida, USA, 865-871.

Berry, A., T. Dabrowski and K. Lyons (2012). The oil spill model OILTRANS and its application to the Celtic Sea. Marine Pollution Bulletin 64, 2489-2501.

Breivik, ∅., J. R. Bidlot and P. A. Janssen (2016). A Stokes drift approximation based on the Phillips spectrum. Ocean Modelling 100, 49-56.

Corn, M. L. (2010). Deepwater Horizon oil spill: coastal wetland and wildlife impacts and response. Diane Publishing, Pennsylvania.

Dagestad, K. F., J. Röhrs, ∅. Breivik and B. Ådlandsvik (2017). OpenDrift v1.0: a generic framework for trajectory modeling. Geoscientific Model Development Discussions, 1-28.

Daniel, P. (1996). Operational forecasting of oil spill drift at Météo-France. Spill Science & Technology Bulletin 3, 53-64.

Daniel, P., F. Marty, P. Josse, C. Skandrani and R. Benshila (2003). Improvement of drift calculation in Mothy operational oil spill prediction system. Proceedings of International Oil Spill Conference, Vancouver, British Columbia, Canada, 1067-1072.

De Dominicis, M., N. Pinardi and G. Zodiatis (2013-Part 1). MEDSLIK-II, a Lagrangian marine oil spill model for short-term forecasting-Part 1: Theory. Geoscientific Model Development Discussions 6, 1949-1997.

De Dominicis, M., N. Pinardi, G. Zodiatis and R. Archetti (2013-Part 2). MEDSLIK-II, a Lagrangian marine oil spill model for short-term forecasting-Part 2: Numerical simulations and validations. Geoscientific Model Development Discussions 6, 1999-2043.

Delvigne, G. A. L. and C. E. Sweeney (1988). Natural dispersion of oil. Oil and Chemical Pollution 4, 281-310.

Fingas, M. (2016). Introduction to spill modeling. In: Oil Spill Science and Technology, edited by K. Hammon, Gulf Professional Publishing, 419-453.

Fingas, M. and B. Fieldhouse (2009). Studies on crude oil and petroleum product emulsions: Water resolution and rheology. Colloids and Surfaces A: Physicochemical and Engineering Aspects 333, 67-81.

Fischer, H. B, E. J. List, R. C. Y. Koh, J. Imberger and N. H. Brooks (1979). Mixing in Inland and Coastal Waters, Academic Press, New York.

Hagerty, C. L. (2010). Deepwater Horizon oil spill: Selected issues for Congress. Diane Publishing, Pennsylvania.

ITOPF (2018). Oil Tanker Spill Statistics 2017. The Iternational Tanker Owners Pollution Federation Limited, London.

Johansen, O. (1982). Drift of submerged oil at sea. Continental Shelf Institute Report No. P319/1, Continental Shelf Institute, Trondheim, Norway.

Johansen, ∅., M. Reed and N. R. Bodsberg (2015). Natural dispersion revisited. Marine Pollution Bulletin 93, 20-26.

Jones, R. (1997). A simplified pseudo-component oil evaporation model. Proceedings of Arctic and marine oil spill program tecnical seminar, 43-62.

Kai, K. Y., F. C. Hao and Y. J. Horng (2017). Grounding of the *T.S. Taipei* in Taiwan. CEDRE Information Bulletin 36, 4-11.

Lehr, W., R. Jones, M. Evans, D. Simecek-Beatty and R. Overstreet (2002). Revisions of the ADIOS oil spill model. Environmental Modelling & Software 17, 189-197.

Li, Z., M. L. Spaulding and D. French-McCay (2017). An algorithm for modeling entrainment and naturally and chemically dispersed oil droplet size distribution under surface breaking wave conditions. Marine Pollution Bulletin 119, 145-152.

Lin, Q. and I. A. Mendelssohn (2012). Impacts and recovery of the Deepwater Horizon oil spill on vegetation structure and function of coastal salt marshes in the northern Gulf of Mexico. Environmental Science & Technology 46,

3737-3743.
Mellor, G. L. (1998). Users guide for a three dimensional, primitive equation, numerical ocean model. Princeton University, Princeton.
Nittis, K., L. Perivoliotis, G. Korres, C. Tziavos and I. Thanos (2006). Operational monitoring and forecasting for marine environmental applications in the Aegean Sea. Environmental Modelling & Software 21, 243-257.
Reed, M., O. M. Aamo and P. S. Daling (1995a). Quantitative analysis of alternate oil spill response strategies using OSCAR. Spill Science & Technology Bulletin 2, 67-74.
Reed, M., ∅. Johansen, P. J. Brandvik, P. Daling, A. Lewis, R. Fiocco, D. Mackay and R. Prentki (1999). Oil spill modeling towards the close of the 20th century: overview of the state of the art. Spill Science & Technology Bulletin 5, 3-16.
Reed, M., O. Johansen, F. Leirvik and B. Brørs (2009). Numerical algorithm to compute the effects of breaking waves on surface oil spilled at sea. Final Report Submitted to the Coastal Response Research Center Report F, 131.
Reed, M. and H. Rye (1995b). A three-dimensional oil and chemical spill model for environmental impact assessment. Proceedings of International Oil Spill Conference, California, USA, 61-66.
Reed, M., I. Singsaas, P. S. Daling, L. G. Faksnes, O. G. Brakstad, B. A. Hetland and J. N. Hofatad (2001). Modeling the water-accommodated fraction in OSCAR2000. Proceedings of International Oil Spill Conference, Florida, USA, 1083-1091.
Sayre, W. W. (1968). A laboratory investigation of open-channel dispersion processes for dissolved, suspended, and floating dispersants. US Government Printing Office, Washington.
Spaulding, M. L. (2017). State of the art review and future directions in oil spill modeling. Marine Pollution Bulletin 115, 7-19.
Stolzenbach, K. D., O. S. Madsen, E. E. Adams, A. M. Pollack and C. K. Cooper (1977). A review and evaluation of basic techniques for predicting the behavior of surface oil slicks. Report No 222. Massachusetts Institute of Technology, Cambridge.
Wang, S. D., Y. M. Shen, Y. K. Guo and J. Tang (2008). Three-dimensional numerical simulation for transport of oil spills in seas. Ocean Engineering 35, 503-510.
Zhang, B., C. Z. Zhang and J. Ozer (1991). SURF-a simulation model for the behavior of oil slicks at sea. Proceedings of The OPERA Workshop, Dalian, China, 61-85.
Zodiatis, G., R. Lardner, D. Solovyov, X. Panayidou and M. De Dominicis (2012). Predictions for oil slicks detected from satellite images using MyOcean forecasting data. Ocean Science 8, 1105-1115.